Experimental observation of ionization and shock fronts in foam targets driven by thermal radiation*

Zhang Ji-Yan(张继彦)[a)†], Yang Jia-Min(杨家敏)[a)], Jiang Shao-En(江少恩)[a)], Li Yong-Sheng(李永升)[b)], Yang Guo-Hong(杨国洪)[a)], Ding Yao-Nan(丁耀南)[a)], Huang Yi-Xiang(黄翼翔)[a)], and Hu Xin(胡 昕)[a)]

[a)] *Research Centre of Laser Fusion, P. O. Box* 919-986, *Mianyang* 621900, *China*
[b)] *Institute of Applied Physics and Computational Mathematics, Beijing* 100088, *China*

(Received 1 May 2009; revised manuscript received 21 May 2009)

The behaviours of ionization and shock propagation in radiatively heated material is crucial for the understanding of indirect drive inertial confinement fusion as well as some astrophysics phenomena. In this work, radiation field with a peak temperature of up to 155 eV was generated in a gold cavity heated by four laser beams on the SG-II laser system and was used to irradiate a plastic foam cylinder at one end. The radiatively ablated foam cylinder was then backlighted side-on by x-ray from a laser-irradiated Ti disk. By observing the transmission decrease due to the shock compression of the foam cylinder, the trajectories of shock front were measured, and from the onset of the intense thermal emission from the side of the cylinder, the propagations of the ionization front were also observed on the same shot. The experimental measurements were compared to predictions of the radiation hydrodynamics code Multi-1D and reasonable agreements were found.

Keywords: ionization wave, shock wave, x-ray radiography

PACC: 5250L, 5235T, 4770M

1. Introduction

Investigations of the interaction of intense radiation with material are of great interest in the fields of astrophysics and inertial confinement fusion studies. In indirect-drive inertial confinement fusion, for example, intense radiation has been used to ablate plastic capsules containing DT fuel and drive the capsule implosion,[1−5] where a precise understanding of the interaction of the x-rays with the outer ablator layer of the fuel capsule is crucial for generating an efficient implosion and subsequent ignition. In the astrophysical domain, radiative shocks have been observed when intense radiation from hot stars interacts with interstellar clouds.[6]

The interaction of intense radiation with material is characterized by the behaviours of ionization and shock propagation in the material.[7−10] When an intense radiation is incident onto cold matter, it first penetrates about a photon mean free path into the material supersonically and creates an ionization front in the matter under the influence of decreasing opacity due to the heating of the matter. Then, if the velocity of the radiation flux is sufficiently high and the material density sufficiently low, this early supersonic period can be extended considerably. Otherwise, the ionization front may propagate transonically or subsonically, depending on both the radiation flux and the material density. In the transonic regime, the ionization front is closely tied to the shock, with the separation of the ionization and shock front less than one radiation mean free path (m.f.p.). In the subsonic regime, the ionization front is overtaken by a shock and forms an ablative heat wave. Supersonic and transonic ionization waves have been observed by backlight techniques[11,12] and the temperature and density profiles were inferred from the transmission contrast between the shocked and unshocked matter.[13] Subsonic heat waves were measured by detecting the delay in the arrival of the burnthrough signal from various sample thicknesses. In this way, radiative burnthrough has been observed in gold foil,[14] Be foil[15] and plastic foil.[16] However, to our knowledge, the propagations of ionization and shock front in these experiments were either measured time-dependently on separate shots, or time-averaged by radiative burnthrough signals, no experiment has ever been performed to measure the ionization and shock front on

*Project supported by the Science and Technology Fund of the China Academy of Engineering Physics (Grant No. 2007B08003).
†Corresponding author. E-mail: zhangjiyanzjy@sina.com
© 2010 Chinese Physical Society and IOP Publishing Ltd

the same shot. So that some of the information that is crucial for the understanding of radiative ablation, for example, the transition of supersonic ionization wave to subsonic ablative wave, has been lost.

In this paper we report the direct measurements of the propagations of radiatively driven ionization and shock front in a plastic foam target on the same shot. The measurements were performed with a time resolved, one-dimensional x-ray radiographic imaging technique, in which the radiation heating and the resulting compression of material were measured both on a shot. In addition, hydrodynamic simulations were also conducted to evaluate the propagations of shock wave and heat wave in the low-density foam by the radiation hydrodynamics code Multi-1D.[17] The calculated results were compared with that from measurements. It should be noted here that plastic foam instead of solid density plastic targets was chosen mainly for two reasons: first, the radiation flux available in this work is not strong and long enough for the ionization wave to propagate in the solid plastic a distance that can be viewed side-on by the x-ray imaging system; second, the low density of foam makes it possible for us to backlight the shock-compressed region with considerable transmission that can be used for diagnostic purpose.

2. Experiment

The experiment was performed on the SG-II laser facility with a half-hohlraum target of 700 μm long and 800 μm in diameter, and a laser entrance hole with a diameter of 380 μm. The hohlraum had an opening at the rear side where a plastic foam sample was mounted. The sample was a plastic (C_8H_8) cylinder of 0.2 mm in diameter and 0.3 mm in length, with a density of (0.16±0.016) g/cm^3. The arrangement of the experiment was illustrated in Fig. 1. Four frequency-tripled beams of the SG-II laser system were used to heat the hohlraum. Each beam carries nominally 260 J of 0.353 μm light in a 1.0-ns duration semi-square laser pulse. The intense x-ray radiation generated in the hohlraum was then used to irradiate the plastic foam cylinder from one end and drive an ionization wave into it. Another two beams of the SG-II laser system, superposed to generated a 1.5-ns duration laser pulse, were focused onto a Ti disk, with an intensity of up to about 2×10^{14} W/cm^2, and formed a $\sim$ 0.4 mm diameter spot. The x-ray emission from the laser-produced Ti plasma was used to backlight the plastic sample at 1.25 ns after the start of the radiative ablation. The delay time is selected under two considerations: first, the x-ray emission imaging of the sample has to be carried out before the backlight beams turn on, when there is not any interference from the backlight source; second, it needs time for the ionization wave to form a shock front in the sample.

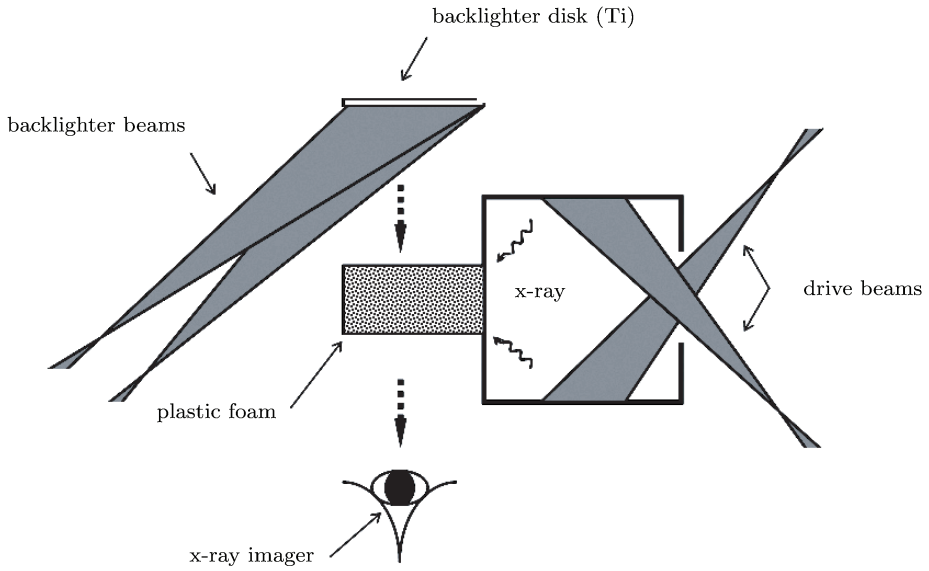


Fig. 1. Schematic plot of the experiment.

Shock compression of the sample increases the areal density, and consequently the optical depth through the sample in the viewing direction, resulting in a decrease in the transmitted backlighter x-ray intensity. In this one-dimensional (1-D) imaging measurement, the sample was viewed side-on by a 15× magnification pinhole imager coupled to an x-ray streak camera. The temporal resolution of the streak camera is about 20 ps. The pinholes are 15 μm in diameter and thus provide about $\sim$ 25-μm spatial resolution. It is worth while noting here that compared to the face-on arrangement, the side-on arrangement provides us with an advantage of not only being able to observe the time-dependent shock propagation, but also to observe the heating wave by the reemission of the heated sample.

3. Radiative hydrodynamic simulation

One-dimensional simulations were performed using the radiation hydrodynamics code Multi-1D. The hydrodynamics code includes multigroup diffusion approximation, flux limited thermal conduction with a flux limiter of 0.03, multigroup opacities calculated from the SNOP code, and tabulated equation of state (EOS) data. The radiation temperature was inferred by flux measurements from the x-ray diode array. The temporal evolution of hohlraum temperature is shown in Fig. 2(a), which was measured by an x-ray diode array and was input into the hydrodynamics code, and the calculated profiles of density and temperature in the foam are illustrated in Fig. 2(b). The simulations show that the ionization wave is closely related to the radiation temperature imposed on the ablation front, and experiences transits from supersonic propagation to transonic propagation and finally subsonic propagation. In the first phase, the ionization wave penetrated into the material supersonically due to the small optical depth, with the shock front lag behind the ionization front, as the case $\Delta t = 250$ ps shown in Fig. 2(b). Then, with the increase in optical depth that ionization wave penetrated into the foam cylinder, the propagation of the ionization front slowed down and was overtaken by the shock front, as the case $\Delta t = 1000$ ps shown in Fig. 2(b). Finally, the ionization front was surpassed by the shock front, as the case $\Delta t = 1750$ ps shown in Fig. 2(b). In fact, no matter what kind of propagation it is, the ionization wave will eventually be surpassed by a shock wave and become ablative, either due to the increase of optical depth or the fall of radiation temperature. A higher radiation flux could only extend the distance of the supersonic propagation. In addition, the transonic ionization wave is only a transit phase and tends to decay to supersonic or subsonic ionization by the radiation flux imposed on the ionization front.

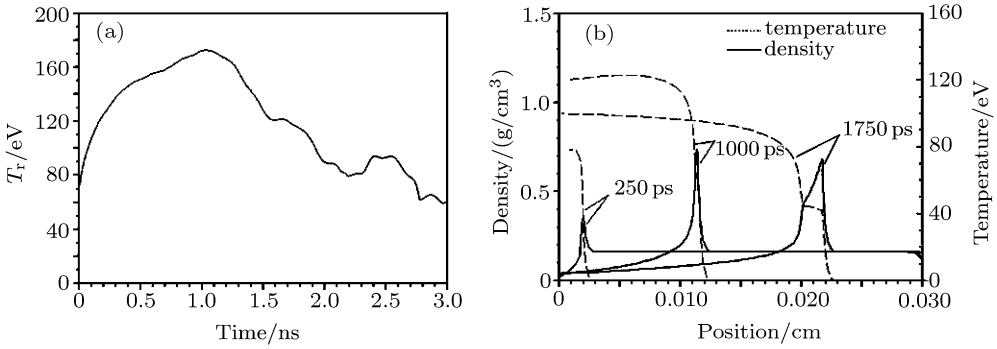


Fig. 2. (a) Time-dependent radiation temperature inferred from the XRD array and (b) the calculated temperature and density profiles in the foam target at three stages in the passage of the ionization front. The drive is incident from the left.

4. Result and discussion

Illustrated in Fig. 3 are the experimentally measured one-dimensional time resolved image of the radiatively heated plastic sample and the simulated trajectory of the target. In Fig. 3(a), a shadow that demonstrates the shock trajectory is clearly seen, and the propagation of ionization front by the sample emission is also observed.

The shock and ionization propagations are qualitatively predicted by the hydrodynamic simulations shown in Fig. 3(b).

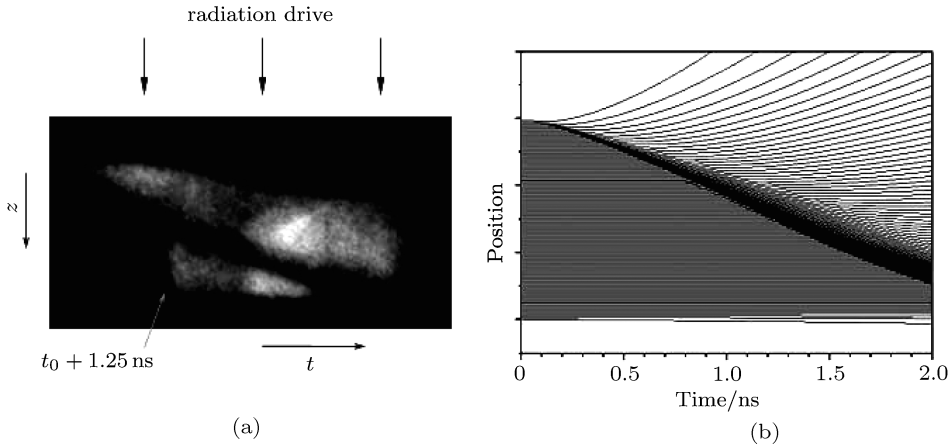


Fig. 3. (a) Shock and ionization front by 1-D radiograph of a shock plastic cylinder of 0.2 mm in diameter and 0.3 mm in length. A streaked 1-D radiographic image of the ablated sample is taken after 1.25 ns after the start of the drive. (b) Calculated trajectories of the foam cylinder by 1-D hydrodynamic code Multi-1D.

In order to compare the results between measurements and the simulations quantitatively, the shock and ionization fronts, were measured experimentally at 50% transmission points and 50% peak-emissivity points, taken from the streak image respectively. The results are compared to predictions of the radiation hydrodynamics code Multi-1D, which is illustrated in Fig. 4. It can be seen from the figure that the measured shock front is consistent with the calculations very well, except some points corresponding to the early phase of the backlight pulse, which we have ascribed to the limited spatial resolution of the 1-D imaging system and the non-uniform backlighter sources at the early phase. However, the measured ionization front does not agree so well with the theoretical calculations since the measured ionization wave is a little slower than the one theoretically predicted. The two-dimensional effects, that is, the transverse radiation leak from the foam cylinder, may be ascribed to the discrepancy from the 1-D radiative hydrodynamic simulations. The uncertainty from experimental measurement is not considered to be an important factor causing the discrepancy. This can be seen in Fig. 5, in which it is shown that the repetivity of the experimental data, i.e. the velocities obtained by fitting linearly the measured ionization fronts from two separate shots, is very good.

Of cause, there may exist other factors that cause this discrepancy, for example, the method used in this work to take the ionization front from the experimental image and the uncertainty from the measurements of the foam densities. Moreover, the uncertainties in opacity and equation of state data may also contribute to the discrepancies. In fact, in some early studies, the opacity data have been adjusted artificially to get a better agreement with the experimental data.

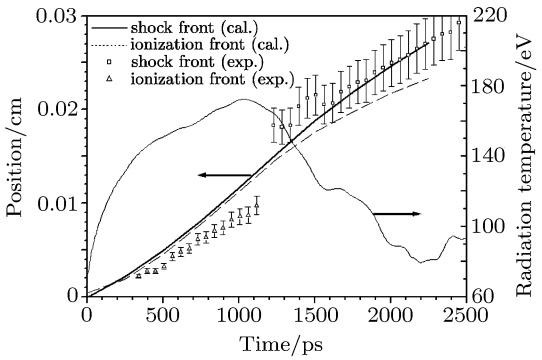


Fig. 4. Comparisons of the observed and calculated propagation characteristics of the ionization wave in the radiative driven foam cylinder. The shock and ionization front are determined by the experimentally observed 50% transmission points. Errors of 10% are added to the experimental data points. Radiative hydrodynamic simulations are conducted using the 1-D code Multi-1D. Radiative temperature used in the simulations is inferred from XRD array detector.

In Fig. 4, errors of 10% have been added to the experimental data points for both the shock and ion-

ization front. These errors may arise mainly from four different sources: 1) spatial resolution of the imaging system, $\sim$ 25 μm, which corresponds to an relative error of 6%; 2) measurement of shock front and reading error, contributing no more than 5% to the total error; 3) calibration of the streak camera sweep, contributing no more than 5% to the total error; 4) streak camera temporal resolution ($\pm$20 ps), contributing no more than 4% to the total error.

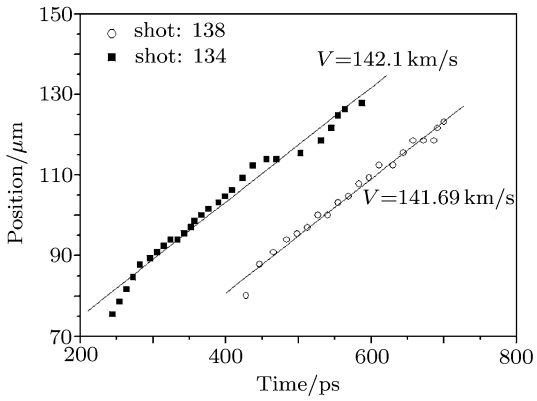


Fig. 5. The trajectories of ionization fronts from two experimental shots.

5. Summary

In conclusion, we have used a 1-D time resolved x-ray radiography to measure the ionization and shock propagation driven by x-ray ablation of low density plastic samples. The trajectories of the ionization and shock front have been observed successfully on the same shot. The experimental data have been compared with theoretical calculations by the hydrodynamic code Multi-1D and reasonable agreements between them have been found.

It should be noted here that the present work gives only the velocities of the ionization and shock fronts. However, to get more information about the radiative ablation of materials, experimental data such as shock compression also has to be measured. New experimental observation using a multispectral monochromatic imaging system has been planned to perform in the future.

Acknowledgements

We thank the SG-II operation staff and the target fabrication staff for their invaluable and dedicated technical assistance. We are also grateful to Ding Yong-Kun, Liu Shen-Ye, Zhang Bao-Han and Zheng Zhi-Jian for their support and encouragement.

References

[1] Lindl J D 1998 *Inertial Confinement Fusion* (New York: Springer-Verlag)
[2] Afsar-rad T, Desselberger M, Dunne M, Edwards J, Foster J M, Hoarty D, Jones M W, Rose S J, Rosen P A, Taylor R and Willi O 1994 *Phys. Rev. Lett.* **73** 74
[3] Olson R E, Leeper R J, Nobile A and Oertel J A 2004 *Phys. Plasmas* **11** 2778
[4] Back C A, Bauer J D, Hammer J H, Lasinski B F, Turner R E, Rambo P W, Landen O L, Suter L J, Rosen M D and Hsing W W 2000 *Phys. Plasmas* **7** 2126
[5] Pasley J, Nilson P, Haines M G, Notley M M, Tolley M, Neely D and Nazarov W 2002/2003 *Central Laser Facility Annual Report*
[6] Drake R P, Carroll III J J, Estabrook K, Glendinning S G, Remington B A, Wallace R and McCray R 1998 *The Astrophysical Journal* **500** L157
[7] Marshak R E 1958 *Phys. Fluids* **1** 24
[8] Zel'Dovich Y B and Raizer Y P 1966 *Physics of Shock Wave and High-Temperature Hydrodynamic Phenomena* (New York: Academic)
[9] Sigel R, Tsakiris G D, Lavarenne F, Massen J, Fedosejevs R, Eidmann K, Meyer-ter-Vehn J, Murakami M, Witkowski S, Nishimura H, Kato Y, Takabe H, Endo T, Kondo K, Shiraga H, Sakabe S, Jitsuno T, Takagi M, Nakai S and Yamanaka C 1992 *Phys. Rev.* A **45** 3987
[10] Kaiser N, Meyer-ter-Vehn J and Sigel R 1989 *Phys. Fluids* B **1** 1747
[11] Hoarty D, Iwase A, Meyer C, Edwards J and Willi O 1997 *Phys. Rev. Lett.* **78** 3322
[12] Hoarty D, Barringer L, Vickers C, Willi O and Nazarov W 1999 *Phys. Rev. Lett.* **82** 3070
[13] Hammer B A, Kilkenny J D, Munro D, Remington B A, Kornblum H N, Perry T S, Phillion D W and Wallace R J 1994 *Phys. Plasmas* **1** 1662
[14] Sigel R, Tsakiris G D, Lavarenne F, Massen J, Fedosejevs R, Meyer-ter-Vehn J, Murakami M, Eidmann K, Witkowski S, Nishimura H, Kato Y, Takabe H, Endo T, Kondo K, Shiraga H, Sakabe S, Jitsuno T, Takagi M, Yamanaka C and Nakai S 1990 *Phys. Rev. Lett.* **65** 587
[15] Schwanda W and Eidmann K 1992 *Phys. Rev. Lett.* **69** 3507
[16] Edwards J, Dunne M, Riley D, Taylor R, Willi O and Rose S J 1991 *Phys. Rev. Lett.* **67** 3780
[17] Ramis R, Schmalz R and Meyer-Ter-Vehn J 1988 *Comput. Phys. Commun.* **49** 475